

OPEN ACCESS

Influence of annealing temperature on the microstructure and mechanical properties of MgB₂

To cite this article: O Gorur *et al* 2009 *J. Phys.: Conf. Ser.* **153** 012012

View the [article online](#) for updates and enhancements.

You may also like

- [Two-band superconductor magnesium diboride](#)
X X Xi
- [Effect of cubic and hexagonal boron nitride additions on the microstructure and properties of bulk MgB₂ superconductors](#)
Zilin Gao, Sangeeta Santra, Chris R M Grovenor *et al.*
- [Fabrication and superconducting properties of internal Mg diffusion processed MgB₂ wires using MgB₂ precursors](#)
Da Xu, Dongliang Wang, Chao Yao *et al.*



245th ECS Meeting • May 26-30, 2024 • San Francisco, CA

Submit now!

Don't miss your chance to present!

Connect with the leading electrochemical and solid-state science network!

Deadline Extended: December 15, 2023



Influence of annealing temperature on the microstructure and mechanical properties of MgB₂

O Gorur¹, M Nursoy², C Terzioglu², A Varilci², I Belenli²

¹ *Department of Physics, Faculty of Arts and Sciences, Rize University, 53100 Rize, Turkey.*

² *Department of Physics, Faculty of Arts and Sciences, Abant İzzet Baysal University, 14280 Bolu, Turkey.*

E-mail: gorur@ktu.edu.tr

Abstract: We have investigated the effect of annealing temperature on the microstructure, magnetic and mechanical properties of MgB₂ superconducting samples employing X-ray diffraction (XRD), scanning electron microscopy (SEM), ac susceptibility and Vickers microhardness measurements. XRD patterns and SEM micrographs are used to obtain information about lattice parameters and grain size, respectively. These measurements indicate that MgB₂ grain size, lattice parameters, and critical temperature are increased, and grain connectivity is improved, with increasing the sintering temperature up to 850°C. It is also observed that the Vickers microhardness of the samples is dependent of the sintering temperature and applied load. In addition, we calculate the load dependent mechanical properties of MgB₂ samples such as the Young's modulus, yield strength, and fracture toughness. The possible reasons for the observed improvements in microstructure, superconducting and mechanical properties due to annealing temperature are discussed.

Keywords: Annealing temperature; Microstructure; Lattice parameters; Ac susceptibility; Microhardness; Fracture toughness; Young's modulus; Yield strength.

1. Introduction

The improvement of the superconducting properties of MgB₂ is a decisive goal to enable its potential applications [1-6]. MgB₂ has been an attractive candidate for various applications due to its relatively high critical current density (J_c), critical temperature (T_c), and coherence length. It is generally known that chemical doping or substitution, and preparation conditions, play very important roles in the properties of high- T_c and conventional superconductors. A number of substitutions into the MgB₂ system have been tried [7-12]. In these investigations, variations in the lattice parameters, microstructure, critical temperature and critical current density with the chemical composition were observed. Variations in these properties were also obtained by changing conditions of sample preparation [13-21]. In a previous study of the present samples, Varilci [22] investigated the influence of magnetic field on hysteretic ac losses in bulk MgB₂ by using Hall probe ac susceptibility. MgB₂ powder is commercially available. Usually its quality is not sufficiently good. The critical temperature of MgB₂ powder prepared in laboratory is slightly higher. On the other hand, even with the same

¹ Osman Gorur, Department of Physics, Faculty of Arts and Sciences, Rize University, 53100 Rize-Turkey.

preparation technique, different research groups observed different values of the critical temperature and the critical current density [15,23].

It is very important to investigate the microstructure and mechanical properties as a function of annealing temperature. To our knowledge, no detailed study of the effect of annealing temperature on mechanical properties of MgB₂ has been published in the literature. In this paper, we report the effects of annealing temperature on the microstructure, superconducting and mechanical properties of MgB₂ by performing XRD, SEM, ac susceptibility and microhardness measurements.

2. Experimental details

A commercially available MgB₂ powder (Alfa Aesar) was used. The powder was pressed into pellets under a pressure of 750 MPa at room temperature and the pellets were wrapped with a Ta foil then placed in a quartz tube for annealing. They were annealed at temperatures of 650 °C, 750 °C, 850 °C and 950 °C for 1 hour in flowing Ar gas [22]. These bulk samples were rectangular bars with approximate dimensions of 10x3x1 mm³. They were analyzed by XRD, SEM, ac susceptibility and microhardness measurements. The MgB₂ pellets will be hereafter denoted as M650, M750, M850, and M950, to indicate their annealing temperature (650 °C, 750 °C, 850 °C, and 950 °C, respectively). The phase composition of the samples were characterized by XRD method using a Jeol Multiflex XRD with Cu K_α radiation ($\lambda = 1.5418 \text{ \AA}$) in the range $2\theta = 30^\circ\text{-}60^\circ$ with a scan speed of 3°/min and a step increment of 0.02° at room temperature. Phase purity and lattice parameters were determined from these XRD patterns. The accuracy in determining the lattice parameters (a and c) was $\pm 0.0001 \text{ \AA}$. The surface morphology and microstructure of the samples were investigated by SEM (JEOL 6390-LV).

Measurements of ac susceptibility were made in the closed cycle refrigerator, using our homemade susceptometer equipped with a lock-in amplifier. A Si diode, attached to the cold head, was used to read the temperature of the sample. The temperature was stabilized with an accuracy of 1 mK. Measurements were taken in the temperature range of 30-45 K with a heating rate of 0.5 K/min using Lake Shore 332S-T1 temperature controller. The real and imaginary components of ac susceptibility were collected with a driving field having amplitude of $H_{\text{app.}} = 960 \text{ A/m}$ and a frequency of 10 Hz. Since the signal generated from the Hall probe was very weak, Tegam model 73 precision ratio transformations was used for voltage amplifier. Details of experimental system were described elsewhere [22,25].

To characterize the mechanical properties of the annealed samples, microhardness measurements were performed with a digital microhardness tester (Instron Series 2100) at room temperature. A Vickers pyramidal indenter with different loads (0.245, 0.490, 0.980, 1.960, and 2.940 N) and a single loading time of 10 s was applied and the diagonals of indentation were measured with an accuracy of $\pm 0.1 \text{ }\mu\text{m}$. Indentations were made at different parts of the samples' surface such that the distance between any two indentations was more than two times the diagonal of the indentation mark to avoid surface effects and work hardening. An average of 5 readings at different locations of specimen surfaces was taken to obtain reasonable mean values for each load.

Conventional Vickers microhardness measurements consist of applying a load F on the test material via a geometrically defined indenter and after the indenter is removed, measuring the characteristic dimension, d , of the resultant impression. The Vickers microhardness, H_v , was estimated using the following equation

$$H_v = 1.8544 \left(\frac{F}{d^2} \right) \quad (1)$$

where F is the load applied (in N) and d the mean diagonal length of the indentation impression (in μm). The scatter in the values of d did not exceed 3%.

In most materials, the elastic modulus (Young's modulus) E is related to the Vickers microhardness (apparent) H_v by the relation [26]

$$E = 81.9635H_v, \quad (2)$$

and yield strength Y is related to the hardness by the relation [27,28]

$$Y \approx H_v/3. \quad (3)$$

In this work, fracture toughness of the annealed MgB_2 samples was measured by Vickers indentation method. Several semi-empirical formulas have been used on the basis of crack types in certain materials [29-33]. Fracture toughness was calculated from the following equation [29]

$$K_{IC} = 0.0016\sqrt{E/H_v} (F/a^{3/2}) \quad (4)$$

where K_{IC} is the fracture toughness in $MPa.m^{1/2}$, F is the applied load in N, E is the Young's modulus in GPa, H_v is the hardness in GPa and a is the crack length in mm.

3. Results and discussion

3.a Lattice parameters and microstructure

The x-ray diffraction patterns taken from the surface of MgB_2 samples (M650, M750, M850 and M950) are shown in Fig. 1. Some of the Miller indices are indicated in the figure. The XRD pattern of sample M950 showed, besides MgB_2 , the presence of a small amount of elemental B (Boron) peaks [17,19]. No traces of MgO or degradation compounds such as MgB_6 or MgB_{12} were observed. The presence of B peaks in the XRD pattern of sample M950 (while being nonexistent in XRD patterns of the other samples) indicates that $950^\circ C$ is too high for heat treating MgB_2 , and may have caused segregation of elemental boron through sublimation of Mg. Since we did not observe any MgO peaks in the XRD patterns, annealing MgB_2 pellets under flowing Ar gas was sufficient enough to avoid partial oxidation of Mg. For samples M650, M750 and M850, only MgB_2 phase was detected [17,19]. The intensity of all peaks increased while the position of the peaks shifted towards smaller angles with increasing the annealing temperatures up to $850^\circ C$ then decreased at $950^\circ C$. The increase of the intensity of the peaks and the decrease of the FWHM with increasing the annealing temperature from 650 to $850^\circ C$ indicate that crystallite size becomes larger as confirmed by SEM investigations. On the other hand, the XRD patterns revealed that all samples show polycrystalline structure with (100), (101), (002.) and (110) peaks.

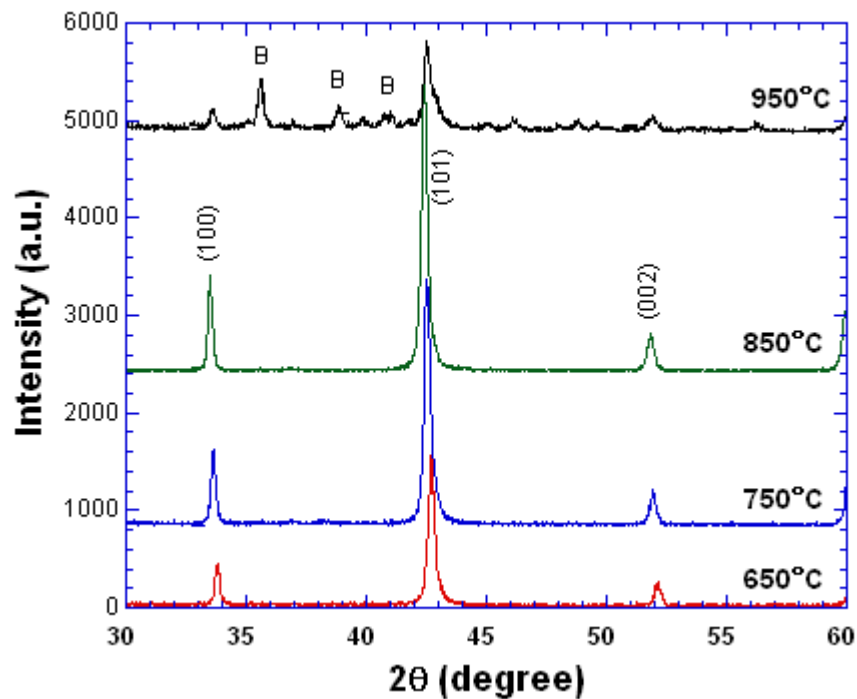


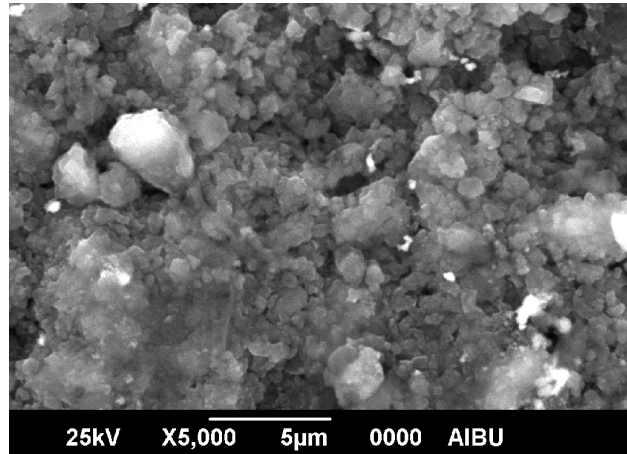
Figure 1. XRD patterns for samples M650, M750, M850 and M950.

The dependence of the lattice parameters on annealing temperature was determined by least-square fits to the position of high angle Bragg peaks ($30^\circ < 2\theta < 60^\circ$) and the results are provided in Table 1. An appreciable change in the lattice parameters of the samples was found within the experimental limit of 0.0001 \AA . The in-plane B-B distance, proportional to the lattice parameter a , increased slightly from 3.0701 to 3.0844 \AA with increasing the annealing temperature up to 850°C . Moreover, the inter-plane B-B distance, proportional to the lattice parameter c , increased significantly from 3.2522 to 3.5285 \AA with increasing the annealing temperature up to 850°C . The lattice parameter c of sample M850 was found to be 3.5285 \AA . On the other hand, it decreased to 3.5090 \AA for sample M950. These lattice parameters are reasonably consistent with other work [34].

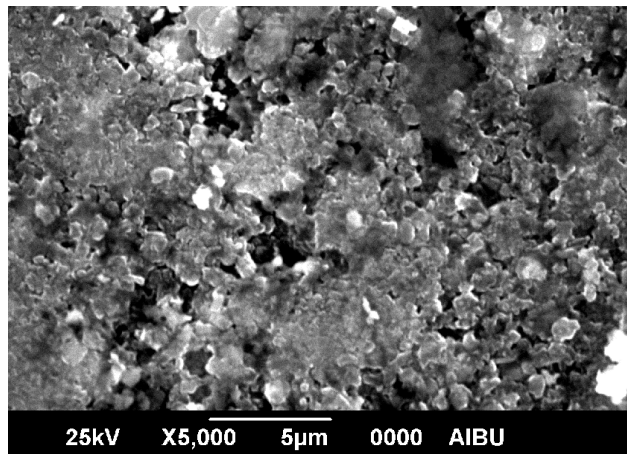
Table 1. The lattice parameters a and c the M950, M850, M750 and M650 samples.

Samples	a (Å)	c (Å)
M950	3.0752	3.5090
M850	3.0844	3.5285
M750	3.0723	3.3522
M650	3.0701	3.2522

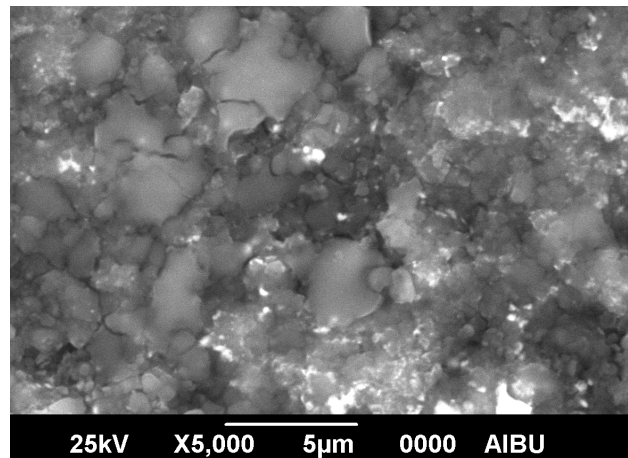
The surface morphology of the four MgB₂ samples was studied by SEM (Fig. 2). The microstructure of the sample annealed at 850 °C is remarkably different from that of samples annealed at 650 and 750 °C.



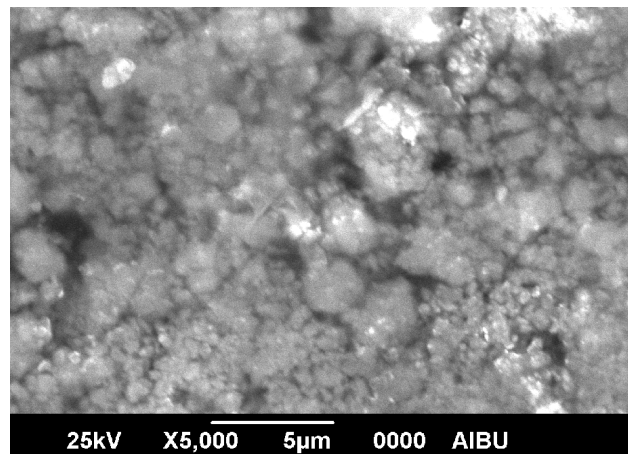
(a)



(b)



(c)



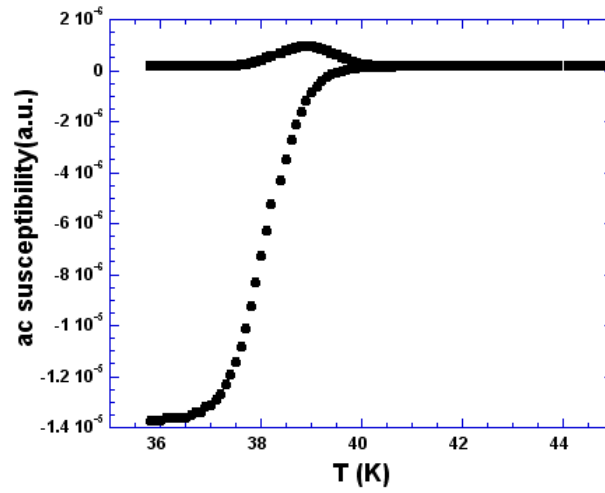
(d)

Figure 2. SEM micrographs of samples (a) M650, (b) M750, (c) M850 and (d) M950.

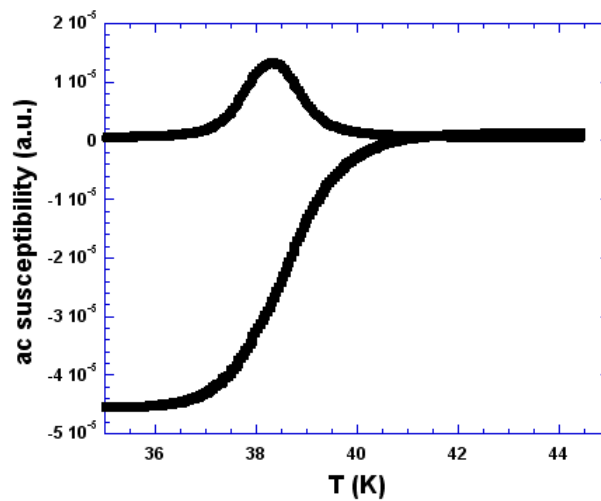
A broad grain size distribution can be seen for the sample annealed at 850 °C. The grain size is about 100-120 nm for sample M850. It is observed that the grain connectivity is enhanced greatly with increasing the annealing temperature from 650 to 850 °C. The surface of sample M850 is also denser. M650 and M750 have a non-uniform surface appearance with smaller grains. From Fig. 2, one can say that the grains in samples M650, M750 are randomly oriented and poorly connected. Grain size of sample M950 is similar to that of M850 but M950 shows more signs of partial melting due to higher annealing temperature. We propose that sublimation of Mg occurred at the grain boundaries where the internal energy of the crystal is higher. As a result, accumulation of segregated boron also occurred at the grain boundaries. This finding is supported by ac susceptibility measurements as explained below.

3.b Critical temperature by ac susceptibility measurements

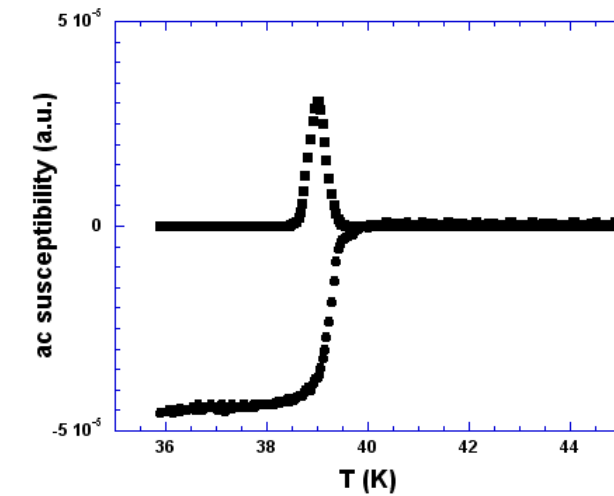
The magnetic ac susceptibility measurements as a function of temperature were made in the temperature range between 35 and 45 K with a driving field having amplitude of $H_{app.} = 960$ A/m and a frequency of 10 Hz. Fig. 3 shows ac susceptibility data as a function of temperature for the four MgB₂ samples annealed at different temperatures.



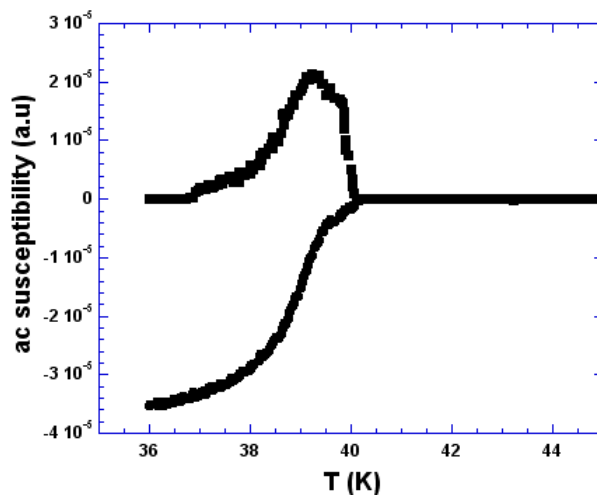
(a)



(b)



(c)



(d)

Figure 3. Temperature dependence of ac susceptibility for samples (a) M650, (b) M750, (c) M850 and (d) M950.

As seen from Fig. 3, sample M850 has a very sharp transition ($\Delta T_c \approx 1 \text{ K}$). All the other samples exhibit wider transitions ($\Delta T_c \approx 3 \text{ K}$). M650 shows a lower T_c due to low annealing temperature.

As the annealing temperature is increased to 750 °C, T_c increased but the transition was still broad. When the annealing temperature increased to 950 °C, the transition widened again. The onsets of T_c of all samples are found to be about 40 K. The broadening could be related to non stoichiometric phases and/or poor sintering between the grains. The shape of the ac susceptibility curves of sample M950 is different from that of the other samples, showing a double step-like behaviour. Double step transitions may indicate the presence of other phases at the grain boundaries indicating that Mg deficient MgB_2 has lower transition temperature. This is consistent with the appearance of boron peaks in the XRD pattern of sample M950.

3.c Mechanical properties

In order to investigate the effect of the annealing temperature on the mechanical properties of MgB₂ samples, we conducted the Vickers microhardness tests. We measured the diagonal length as a function of the test load. The Vickers microhardness (apparent) values, calculated for different applied loads by using Eq. (1), are listed in Table 2.

Table 2. Load dependent micro hardness, elastic modulus, yield strength and fracture toughness of MgB₂ samples annealed at 650, 750, 850 and 950 °C.

Sample	Load (N)	H_v (GPa)	E (GPa)	Y (GPa)	K_{IC} (MPa \sqrt{m})
M650	0.245	1.011	82.86	0.337	4.005
	0.490	0.682	55.90	0.227	3.806
	0.980	0.537	43.96	0.179	3.787
	1.960	0.502	41.14	0.167	3.539
	2.940	0.494	40.45	0.165	3.874
M750	0.245	2.568	210.5	0.856	8.321
	0.490	1.228	100.7	0.409	6.301
	0.980	0.863	70.70	0.288	5.883
	1.960	0.791	64.81	0.264	5.142
	2.940	0.780	63.94	0.260	4.762
M850	0.245	3.824	313.4	1.275	12.55
	0.490	1.674	137.2	0.558	8.488
	0.980	1.065	87.33	0.355	7.348
	1.960	0.952	78.00	0.317	5.711
	2.940	0.944	77.37	0.315	5.352
M950	0.245	1.450	118.9	0.483	6.830
	0.490	0.917	75.06	0.305	6.349
	0.980	0.721	59.11	0.240	5.728
	1.960	0.658	53.96	0.219	5.420
	2.940	0.628	51.80	0.208	5.142

Fig. 4 displays the variation of microhardness as a function of applied load for samples M650, M750, M850 and M950. These MgB₂ samples have higher mechanical strength than the other high-T_c ceramic superconductors (YBaCuO and Bi(Pb)SrCaCuO) [5,6,11,35].

The variation of microhardness with load has similar shape irrespective of the annealing temperature although its value for a given load is different depending on the annealing conditions. We have observed that the microhardness values increased with increasing annealing temperature from 650 to 850 °C, and decreased at 950 °C. At 950 °C, the strength of bonding between the grains decreased and consequently the microhardness degraded. The rapid variation of microhardness was observed with increasing applied load from 0.245 to 1.000 N. The reason for this behaviour is due to mechanically weak grain boundaries [36]. It is also obvious from Fig. 4 that the Vickers microhardness is load dependent for all samples; the calculated microhardness decreased non-linearly as the applied load increased until 1 N, and then attained saturation. The reason of this behaviour is explained elsewhere [37]. This non-linearity has also been observed for *Bi-Pb-Sr-Ca-Cu-O* [38-40] and for MgB₂ [5,6], and is known as indentation size effect (ISE). To account for this effect, several relationships between the applied load and the resulting indentation size have been suggested [41-44]. However, we are not going to analyze the ISE in this paper, but will focus on the load dependent mechanical properties. Quin et al. [45] investigated the variation of the Vickers microhardness as a function of the indentation load for a variety of ceramic materials. They observed that such hardness-load curve shows distinct

transition to a plateau and concluded that this plateau corresponds to the intrinsic hardness value of the material. In this study, this plateau is reached at an applied load of about 1 N. It is evident that the value of microhardness of sample M850 is larger than that of the other samples. This result is consistent with XRD, SEM and ac susceptibility measurements.

The value of load dependent E , Y , and K_{IC} were calculated for each load by using Eqs. (2) and (4), and summarized in Table 2. As seen in this table, the load dependent E , Y and K_{IC} increase significantly with increasing annealing temperature and decreasing loads.

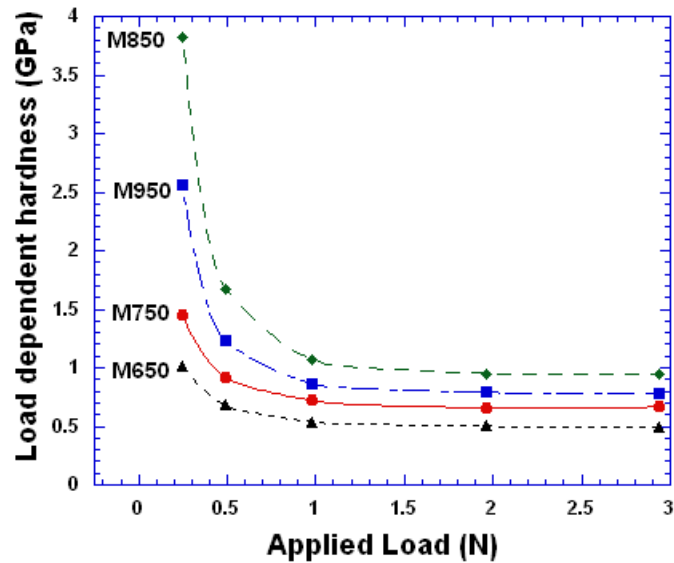


Figure 4. Load dependent microhadness versus applied load for the samples.

Similar changes in the yield strength, elastic modulus and fracture toughness were reported in the literature [46-48]. An increase in K_{IC} corresponds to an increase in the average surface energy as proposed from the hardness calculations. One should point out that the apparent microhardness, Young's modulus, yield strength, and fracture toughness of the samples in the present work indicate strong dependency on applied load and weak dependency on annealing temperature. It was observed that the mechanical properties of the samples are improved with increasing the annealing temperature from 650 to 850 °C (Fig. 5). At 950 °C, however, the mechanical properties showed a significant decrease. This indicates that the optimum annealing temperature to harden MgB_2 material is around 850 °C.

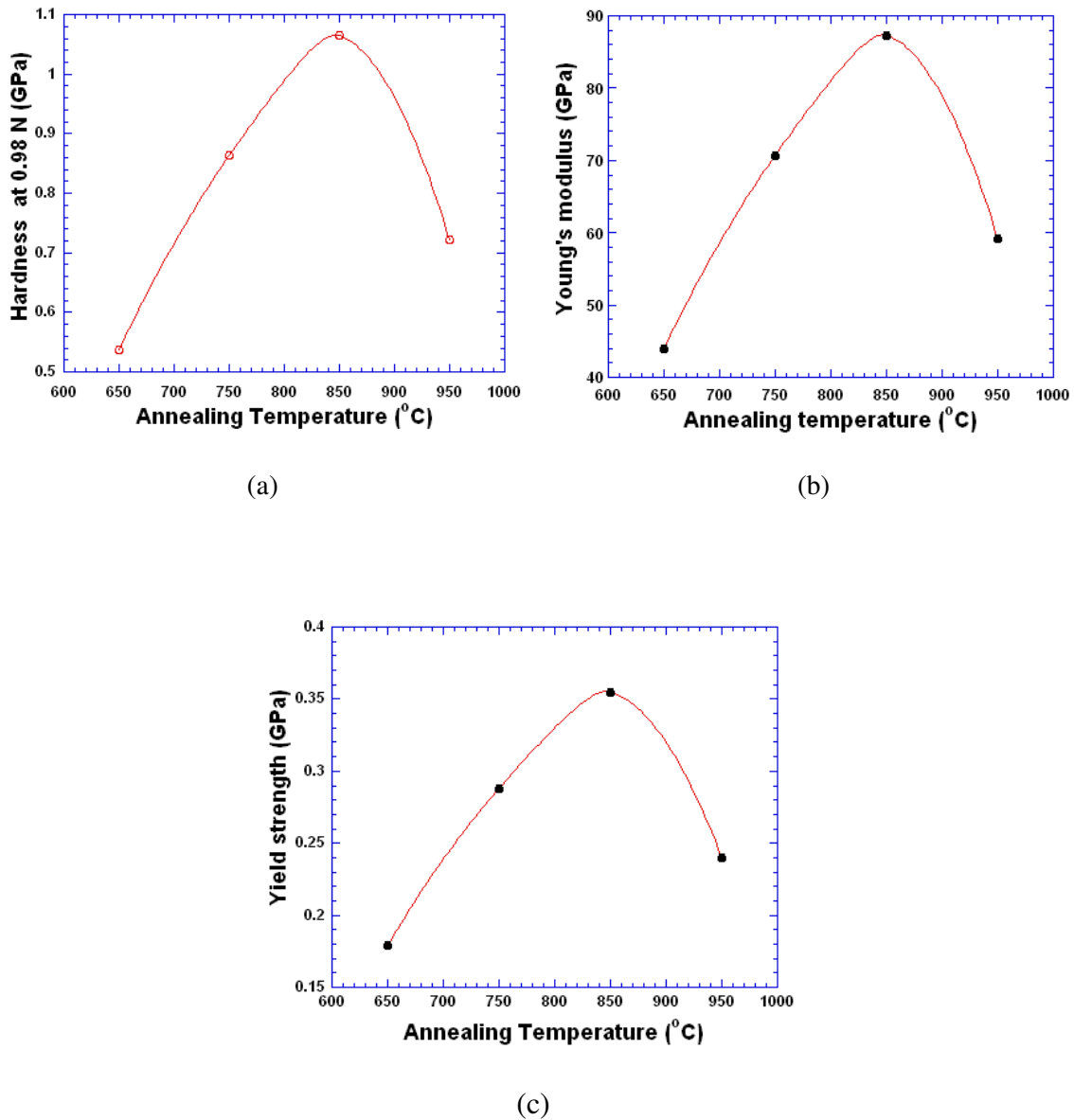


Figure 5. (a) Hardness, (b) Elastic modulus, and (c) Yield strength versus annealing temperature at 0.98 N.

4. Conclusions

Our measurements showed that an increase in the annealing temperature up to 850°C improved the microstructure, mechanical and superconducting properties of MgB₂ bulk samples. XRD and SEM examinations show that the lattice parameters and grain connectivity increase, and the number and size of voids at the sample surface decrease with increasing the annealing temperature from 650 to 850 °C. As a result, load dependent microhardness, elastic modulus, yield strength and fracture toughness values increase with increasing the annealing temperature. It was also found that the hardness of MgB₂ samples is greater than that of high-T_c ceramic superconductors (YBaCuO and Bi(Pb)SrCaCuO). The improvement of the superconducting properties (T_c and transition width) with increasing the annealing

temperature is due to the modification of grain boundaries together with a better crystallinity and larger grains. The improvement of the mechanical properties can be observed by the increase of microhardness with increasing annealing temperature. The mechanical properties enhanced with increasing the annealing temperature, up to 850 °C and degraded at 950 °C. This behaviour is ascribed to the strength of the bonds between grains. The higher annealing temperature raised the reactivity for the formation of MgB₂ phase. We conclude that the best annealing temperature of these MgB₂ samples is 850 °C.

Acknowledgements

One of the authors, Ahmet Varilci, would like to thank to the Turkish State Planning Organization (DPT) for its financial support (project No: 2004K120200).

References

- [1] Sou H L, Benedence C, Dhall M, Musolino N, Genound J Y, Flükiger R 2001 *Appl. Phys. Lett.* **79** 3116
- [2] Anderson N E, Straszheim W E, Bud'ko S L, Canfield P C, Finnemore D K, Suplinskas R J 2003 *Physica C* **390** 11
- [3] Zhao Y, Cheng C H, Feng Y, Machi T, Huang D X, Zhou L, Koshizuka N, Mukrakami M 2003 *Physica C* **386** 581
- [4] Vilke R H T, Bud'ko S L, Canfield P C, Kramer M J, Wu Y Q, Finnemore D K, Suplinskas R J, Marzik J V, Hannahs S T 2005 *Physica C* **418** 160
- [5] Kolemen U 2006 *J. Alloys Comp.* **425** 429
- [6] Kolemen U, Uzun O, Aksan M A, Güçlü N, Yakıncı E 2006 *J. Alloys Comp.* **415** 294
- [7] Xu X L, Guo J D, Wang Y Z, Wang X 2003 *Materials Letters* **58** 142
- [8] Tampieri A, Celotti G, Sprio S, Rinaldi D, Baruccai G, Caciuffo R 2002 *Solid State Comm.* **121** 497
- [9] Gencer A, Kılıç A, Okur S, Güçlü N, Özyüzer L and Belenli I 2005 *IEEE Transactions on Applied Superconductivity* **15(2)** 3352
- [10] Kazakov S M, Angst M, Karpinski J, Fita I M, Puzniak R 2001 *Solid State Comm.* **119** 1
- [11] Hong-xia L, Hong-wei S, Gou-xing L, Chang-ping C 2005 *Ceramic International* **31** 105
- [12] Güçlü N 2007 *Materials Chemistry and Physics* **101** 470
- [13] Kolesnikov N N, Kulakov M P 2001 *Physica C* **363** 166
- [14] Takano H, Kokubo H, Kinami T, Amakai Y, Murayama S 2007 *Journal of Magnetism and Magnetic materials* **310** e134
- [15] Wu T, Yau J K F, Cai Y M, Cui Y G, Gu D W, Yuan P F, Yuan G Q, Shen L J, Jin X 2003 *Physica C* **386** 638
- [16] Yamamoto A, Shimoyama J, Ueda S, Katsura Y, Iwayama I, Horii S, Kishio K 2005 *Physica C* **426-431** 1220
- [17] Qing-rong F, Chinping C, Jun X, Ling-wen K, Xin C, Yong-zhong W, Yan Z, Zheng-xiang G 2004 *Physica C* **411** 41
- [18] Matsumoto A, Kumakara H, Kitaguchi H, Fuji H, Tugano K 2002 *Physica C* **382** 207
- [19] Aswal D K, Sen S, Singh A, Chandrasekhar Rao T V, Vyas J C, Gupta L C, Sahni V C 2001 *Physica C* **363** 149
- [20] Xu G J, Pinholt R, Bilde-Sorensen J, Grivel J C, Abrahamsen A B, Andersen N H 2006 *Physica C* **434** 67
- [21] Abe H, Naito M, Nogi K, Matsuda M, Miyake M, Ohara S, Kondo A, Fukui T 2003 *Physica C* **391** 211
- [22] Varilci A 2007 *Supercond. Sci. Technol.* **20** 397
- [23] Buzea C, Yamashita T 2001 *Supercond, Sci, Technol.* **14** R115
- [24] Cullity B D 1978 *Element of X-ray diffraction, Addition* – Wesley, Reading, MA

- [25] Yegen D Varilci A Yilmazlar M Terzioglu C Belenli I 2007 *Physica C*
- [26] Veerender C Dumke V R Nagabhooshanam M 1994 *Phys. Status Solid A* **144** 199
- [27] McClintock F A Argon A S 1996 *Mechanical Behaviour of Materials*, Addison-Wesley, Reading, MA, (p. 455)
- [28] Tabor D 1951 *The Hardness of Metals*, Clarendon, Oxford
- [29] Anstis GR Chantikul P Lawn B R and Marshall D B 1981 *J. Am. Ceram. Soc.*, **64** 533-538
- [30] Evans A F Wilshaw T R 1976 *Acta Met.* **24** 939
- [31] Liang K M 1990 *J. Mater. Sci.* **25** 207
- [32] Austis G R 1994 *J. Am. Ceram.* **64** 533
- [33] Habib K A Saura J J Ferrer C Damra M S Gimenez E Cabedo L 2006 *Surface & Coatings Technology* **201** 1436.
- [34] Drozd V A Gabovich A M Gierłowski P Pezkała M Szymczak H 2004 *Physica C* **402** 325
- [35] Beilin V Dul'kin E Yashchin E Galstyan E Lapides Y Tsindlekht M Felner I Roth M 2004 *Physica C* **405** 70
- [36] Ling H C and Yan M F 1988 *J. Appl. Phys.* **64** 1307
- [37] Rabier J Denanot M F 1990 *J. Less Common Met.* **223** 164
- [38] Yilmazlar M Cetinkara H A Nursoy M Ozturk O and Terzioglu C 2006 *Physica C* **442** 101
- [39] Khalil S M 2001 *J. Phys Chem Solids* **62** 457
- [40] Murakami A Katagiri K Noto K Kasaba K Sohoji Y Muralidhar M Sakai N and Murakami M 2002 *Physica C* **378-381** 794
- [41] Fröhlich F Grau P Grellmann W 1997 *Phys. Status Solidi* **42** 79
- [42] Li H Bradt R C 1993 *J. Mater. Sci.* **22** 917
- [43] Hays C Kendall E G 1973 *Metallography* **6** (4) 275
- [44] Gong J Wu J Guan Z 1999 *J. Eur. Ceram. Soc.* **19** 2625
- [45] Quinn J B Quinn G D 1997 *J. Mater. Sci.* **32** 4331
- [46] Khalil SM 2005 *Smart Mater. Struct.* **14** 804
- [47] Veerender C Dumke V R Nagabhooshanam M 1994 *Phys. Status Solid A* **144** 199
- [48] Goyal A Funkenbusch P D Kroeger D M Burns S J 1992 *J. Appl. Phys.* **71** 1363